Supporting Information

Tuning catalysis of boronic acids in microgels by in situ reversibly structural variations

Zhenghao Zhai,[a,‡] Xue Du,[a,‡] Qingshi Wu,[b] Lin Zhu,[a] Zahoor H. Farooqi,[c] Jin Li,[a] Ruyue Lan,[a] Yusong Wang[d] and Weitai Wu*[a]

[a] *State Key Laboratory for Physical Chemistry of Solid Surfaces, Collaborative Innovation Center of Chemistry for Energy Materials, and Department of Chemistry, College of Chemistry and Chemical Engineering, Xiamen University, Xiamen, Fujian 361005, China*
[b] *College of Chemical Engineering and Materials Science, Quanzhou Normal University, Quanzhou, Fujian 362000, China*
[c] *Institute of Chemistry, University of the Punjab, New Campus, Lahore 54590, Pakistan*
[d] *Hefei National Laboratory for Physical Sciences at the Microscale, University of Science and Technology of China, Hefei, Anhui 230026, China*

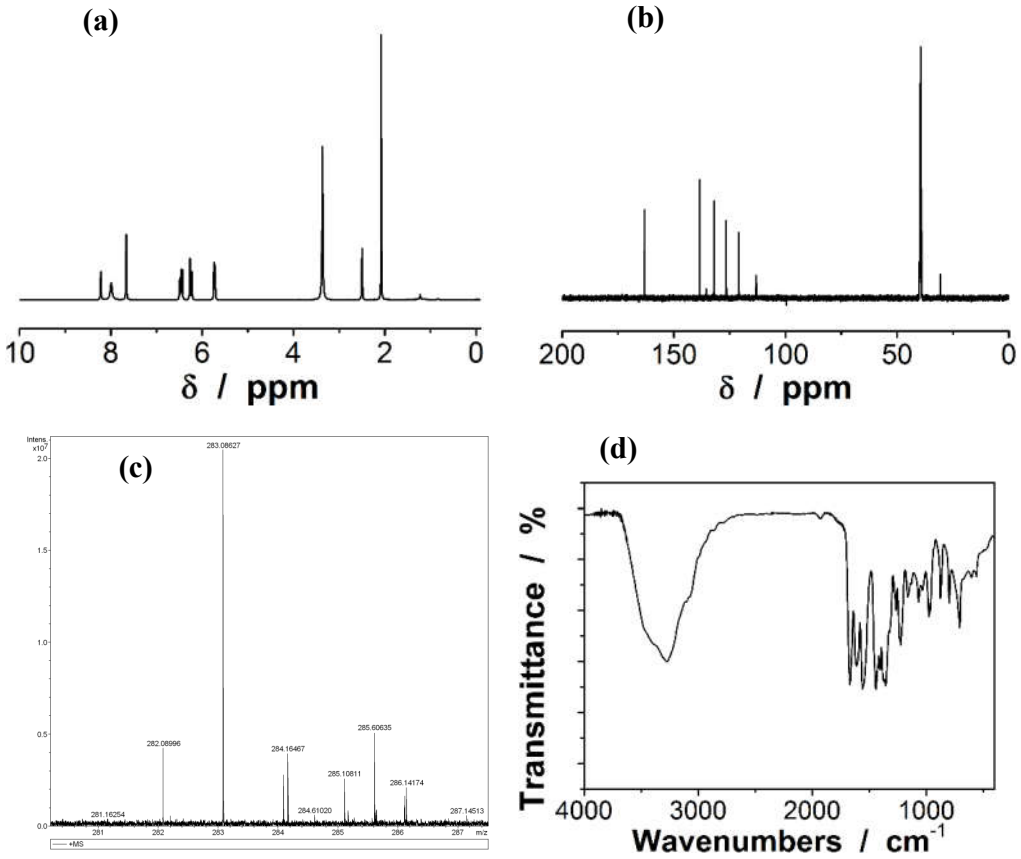

Fig. S1. (a) ^{1}H NMR (in DMSO-d6), (b) ^{13}C NMR (in DMSO-d6), (c) FT-MS, and (d) IR spectra of **1**. ^{1}H NMR: δ = 10.10 (2H, N*H*), 8.22 (1H, Ar*H*), 7.99 (2H, B(O*H*)$_2$), 7.67 (2H, Ar*H*), 6.47

(2H, C*H*=CH_2), 6.25 (2H, CH=CH_2), 5.73 (2H, CH=CH_2); ^{13}C NMR: δ = 113.14, 120.90, 126.53, 132.05, 135.51, 138.42, 163.10; FT-MS: m/z 283.09 [M+Na^+].

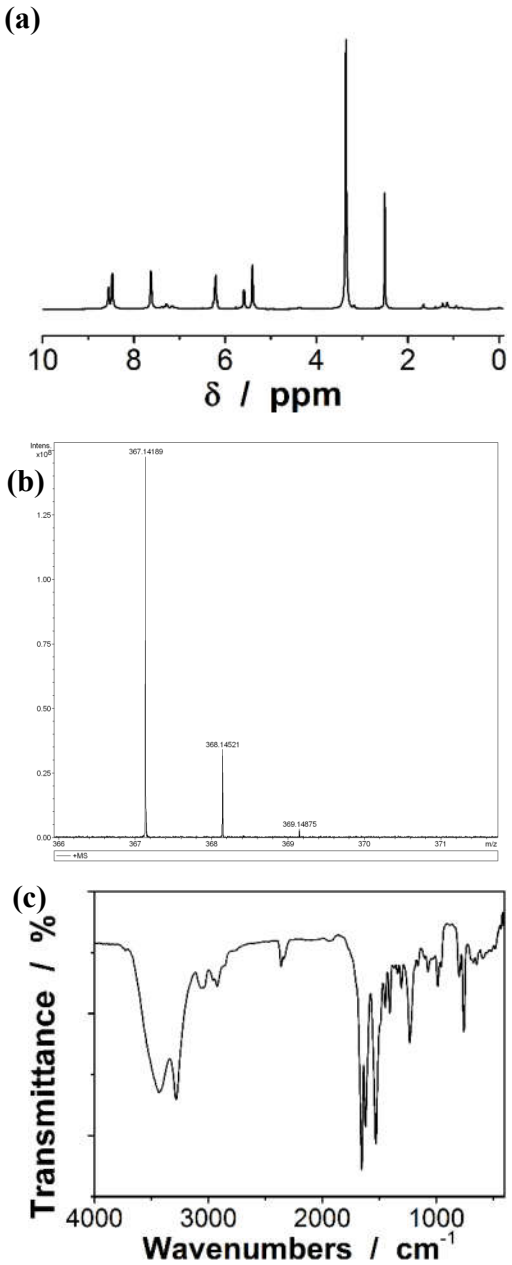

Fig. S2. (a) ^{1}H NMR (in DMSO-d6), (b) FT-MS, and (c) IR spectra of **2**. ^{1}H NMR: δ = 8.56 (2H, N*H*), 8.48 (4H, Ar*H*), 7.63 (2H, Ar*H*), 6.21 (4H, ArCH_2), 5.59 (2H, C*H*=CH_2), 5.40 (4H, CH=CH_2); FT-MS: m/z 367.14 [M+Na^+].

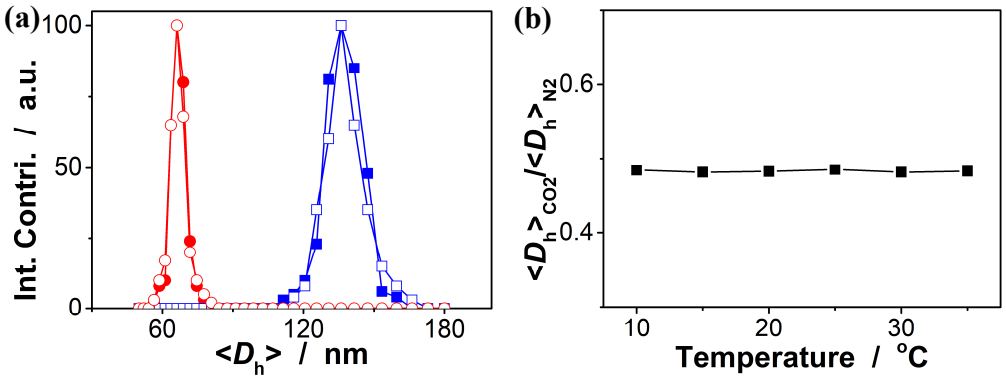

Fig. S3. (a) DLS size distribution of the PBA@PM in CH_2Cl_2/water (9:1 in volume) upon heating (to 35.0 °C; ■,●) or cooling (to 10.0 °C; □,○) and bubbling with N_2 (■,□) or CO_2 (●,○) gas. (b) Influence of the solution temperature on the $\langle D_h \rangle_{CO2}/\langle D_h \rangle_{N2}$, where the $\langle D_h \rangle_{CO2}$ and the $\langle D_h \rangle_{N2}$ were measured on the same microgels at the same temperature upon bubbling with N_2 or CO_2 gas correspondingly.

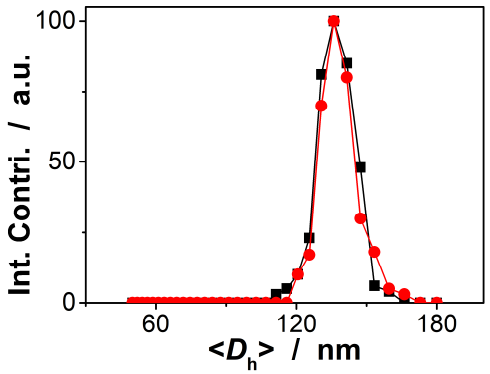

Fig. S4. DLS size distribution of the PBA@PM (■) in CH_2Cl_2/water (9:1 in volume) before and (●) after 6 months' storage under the N_2 atmosphere at 10.0 °C.

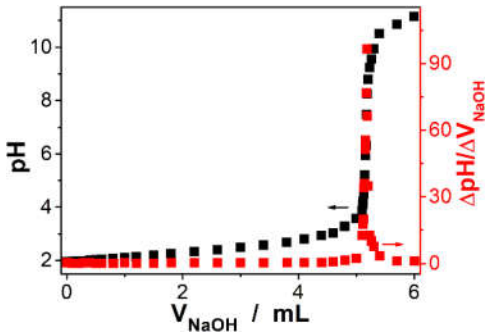

Fig. S5. Titration curve of the PBA@PM using 10.0 mM NaOH solution. All measurements were made at 10.0 °C.

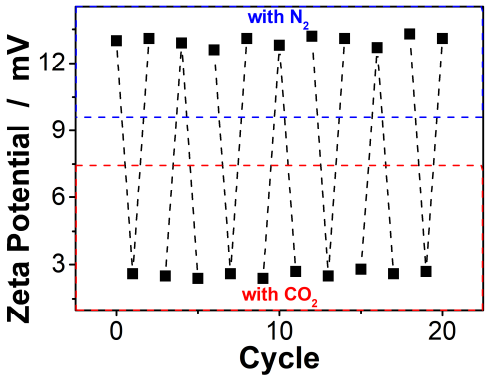

Fig. S6. The zeta potential of the PBA@PM dispersed in CH_2Cl_2/water (9:1 in volume) upon bubbling with N_2 or CO_2 gas.

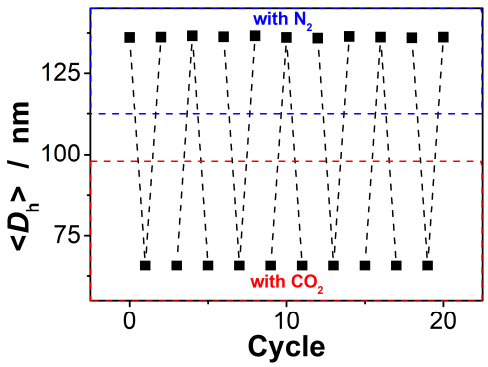

Fig. S7. The $<D_h>$ of the PBA@PM dispersed in CH_2Cl_2/water (9:1 in volume) upon bubbling with N_2 or CO_2 gas.

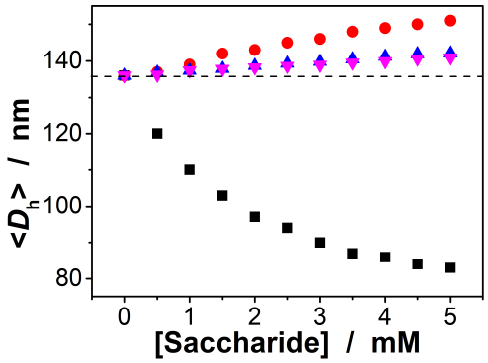

Fig. S8. [Saccharide]-dependent $<D_h>$ of the PBA@PM in CH_2Cl_2/water (9:1 in volume) under the N_2 atmosphere at 10.0 °C, upon adding glucose (■), fructose (●), galactose (▲) or mannose (▼).

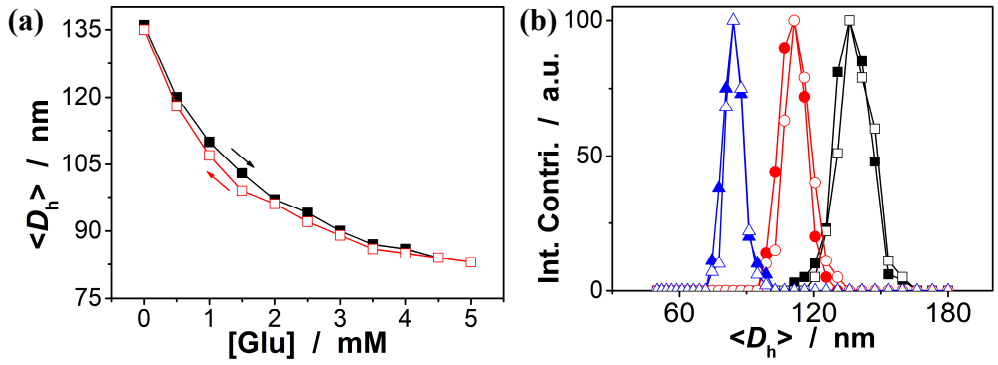

Fig. S9. (a) [Glu]-dependent <D_h> of the PBA@PM dispersed in CH_2Cl_2/water (9:1 in volume) under the N_2 atmosphere at 10.0 °C. (b) DLS size distribution of the PBA@PM before (solid symbols) and after (open symbols) five cycles of adding ([Glu] = 1.0 mM: ●,○; [Glu] = 5.0 mM: ▲,Δ) and removing ([Glu] = 0.0 mM: ■,□) glucose by dialysis.

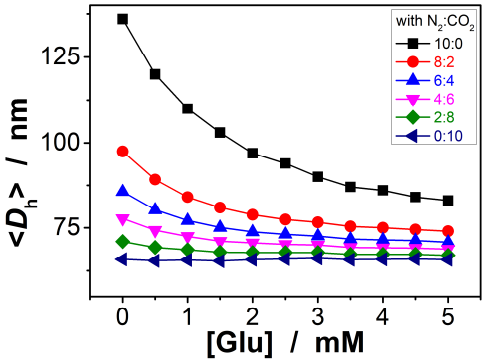

Fig. S10. Glucose-dependent <D_h> of the PBA@PM dispersed in CH_2Cl_2/water (9:1 in volume) upon bubbling with gases containing appropriate amount (in volume) of CO_2 gas, measured at 10.0 °C and at a scattering angle of 45°.

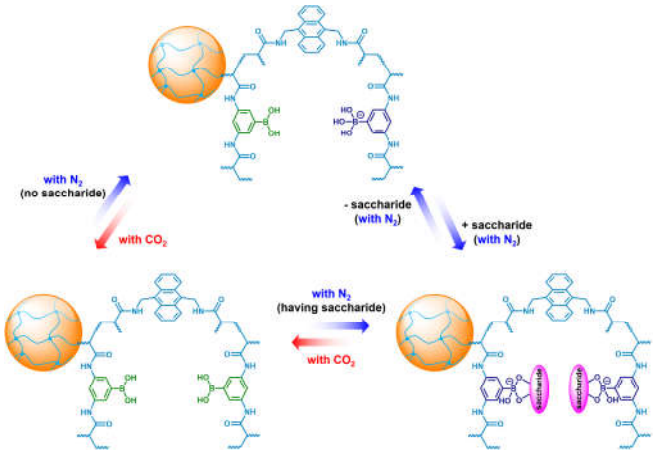

Fig. S11. A possible mechanism on structural modifications in the PBA@PM upon bubbling with N_2/CO_2 gases, in the presence or absence of fructose, galactose or mannose.

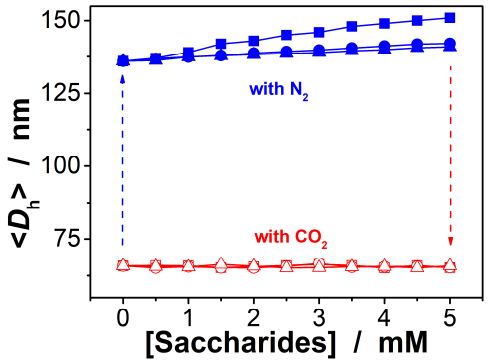

Fig. S12. [Saccharides]-dependent <D_h> of the PBA@PM in CH_2Cl_2/water (9:1 in volume) at 10.0 °C, upon adding fructose (■,□), galactose (●,○) or mannose (▲,△) and bubbling with N_2 or CO_2 gas.

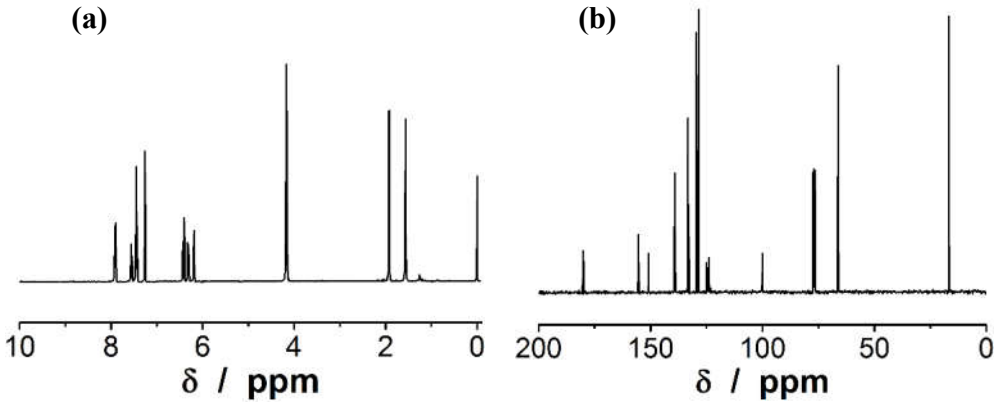

Fig. S13. (a) ^{1}H NMR (in $CDCl_3$) and (b) ^{13}C NMR (in $CDCl_3$) spectra of **3**. ^{1}H NMR: δ = 7.91 (2H), 7.56 (1H), 7.44 (2H), 6.42 (1H), 6.31 (1H), 6.19 (1H), 4.17 (4H), 1.92 (3H); ^{13}C NMR: δ = 180.3, 155.6, 150.9, 139.4, 133.4, 133.1, 129.6, 128.7, 125.0, 124.1, 100.2, 66.4, 16.9.

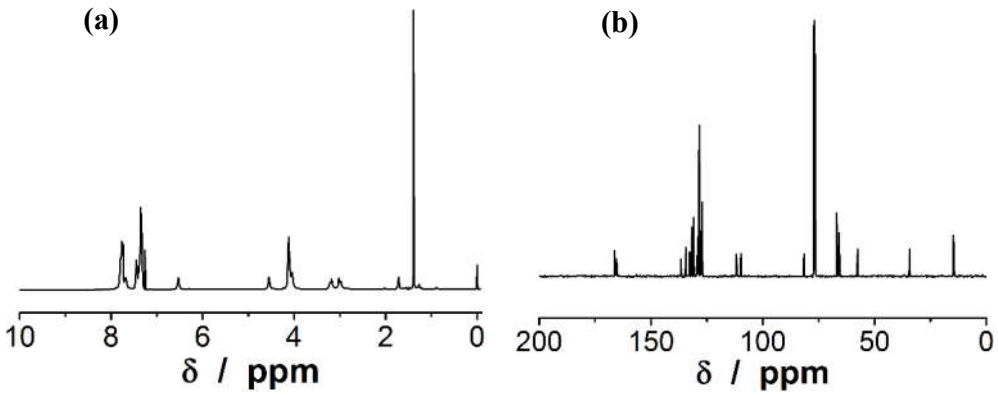

Fig. S14. (a) ^{1}H NMR (in $CDCl_3$) and (b) ^{13}C NMR (in $CDCl_3$) spectra of product **6**. ^{1}H NMR: δ = 7.80-7.74 (4H), 7.66 (1H), 7.48-7.30 (6H), 6.52 (1H), 4.55 (1H), 4.13-4.03 (4H), 3.20 (1H), 3.01 (1H), 1.38 (3H); ^{13}C NMR: δ = 166.2, 165.6, 136.5, 134.6, 132.8, 131.8, 130.8, 129.2, 128.3, 127.7, 127.1, 112.1, 109.7, 81.6, 66.8, 65.7, 57.7, 34.5, 14.6.

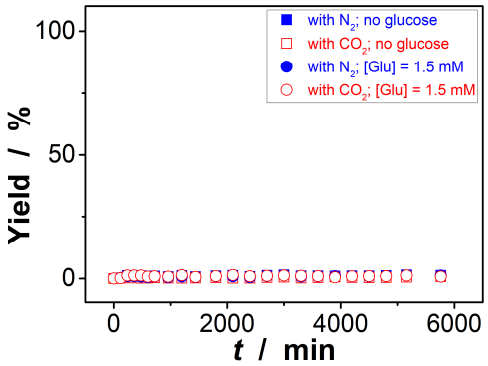

Fig. S15. Time trace of the yield of **6** of the reaction at 10.0 °C, without any organoboron acid catalysts.

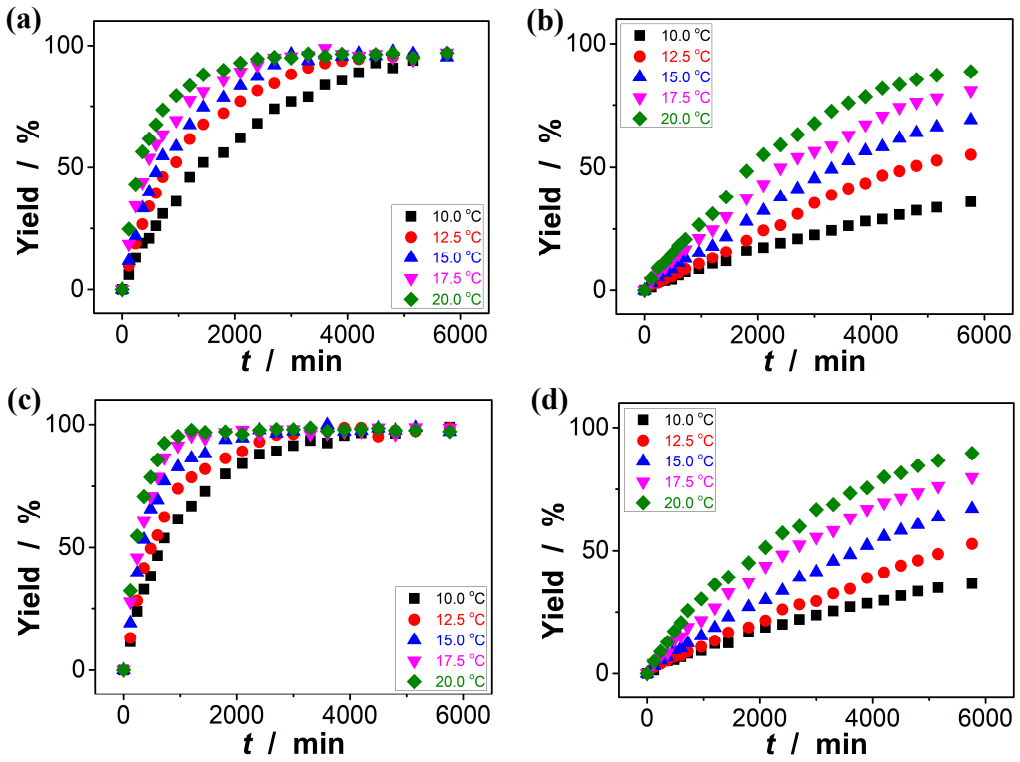

Fig. S16. Time trace of the yield of **6** of the reaction catalyzed by the PBA@PM in the absence (a,b) or presence (c,d) of glucose (1.5 mM), upon bubbling with N_2 (a,c) or CO_2 (b,d) gas.

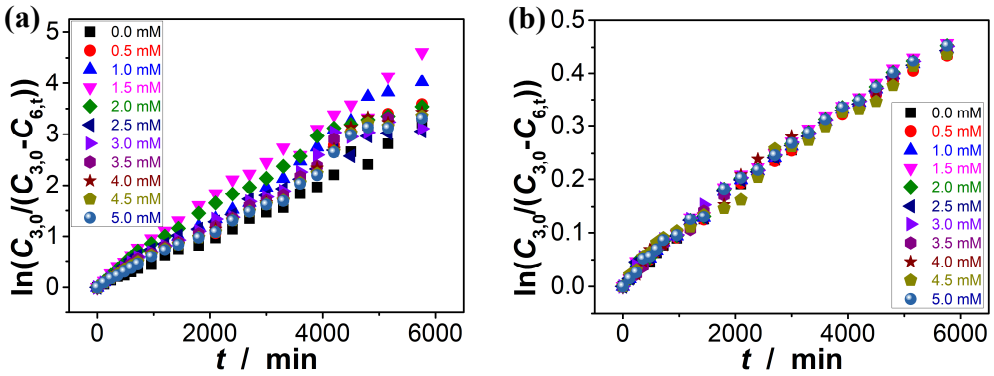

Fig. S17. Influence of the [Glu] on the *k*, measured in the reaction mixture upon bubbling with (a) N_2 or (b) CO_2 gas at 10.0 °C.

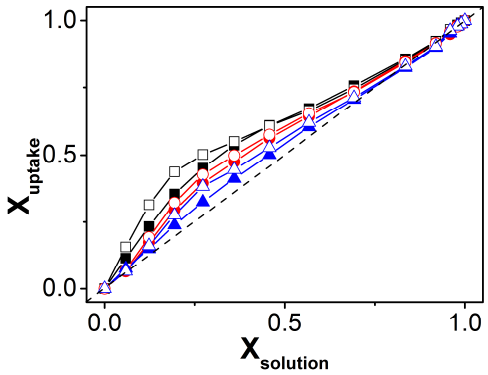

Fig. S18. A comparison of the uptaken mol fraction of **3** (■, [Glu] = 0.0 mM; ●, [Glu] = 1.5 mM; ▲, [Glu] = 5.0 mM), or **4** (□, [Glu] = 0.0 mM; ○, [Glu] = 1.5 mM; Δ, [Glu] = 5.0 mM), in the equilibrated PBA@PM at 10.0 ºC, and corresponding mol fraction in initial solutions.

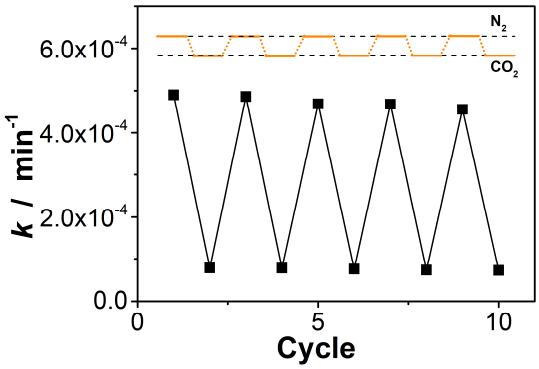

Fig. S19. A comparison of the catalysis activity of the PBA@PM upon repeated bubbling with N_2 or CO_2 gas, measured at 10.0 ºC without glucose.

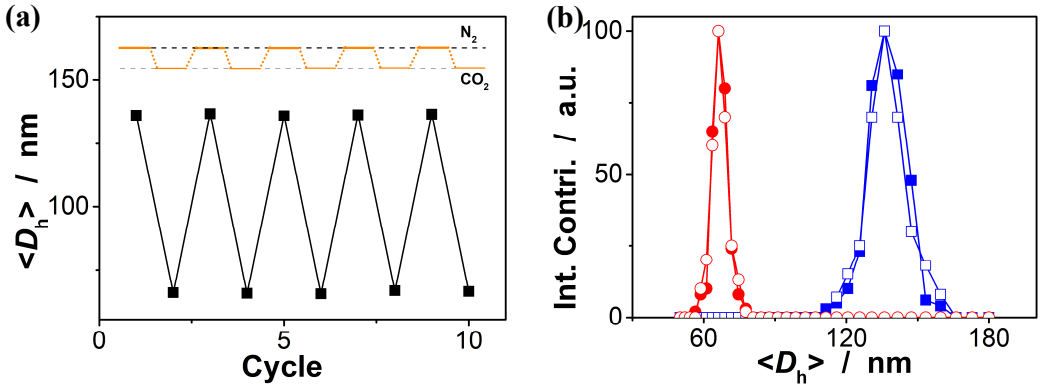

Fig. S20. (a) A comparison of the <D_h> of the PBA@PM upon repeated use in the reaction bubbling with N_2 or CO_2 gas. (b) DLS size distribution of the PBA@PM before (■,●) and after (□,○) ten cycles of use as catalyst and bubbling with N_2 (■,□) or CO_2 (●,○) gas. The reused PBA@PM was collected after each reaction and purified for DLS measurements at 10.0 ºC.

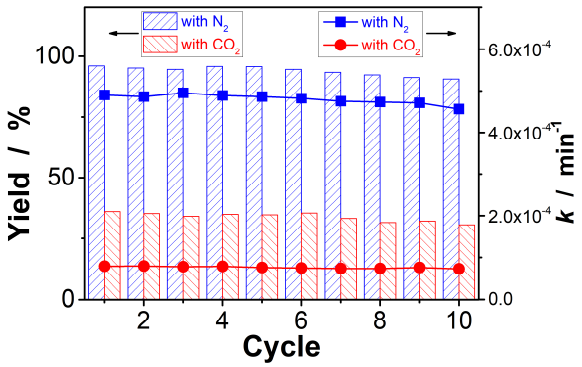

Fig. S21. A comparison of the catalysis activity of the PBA@PM upon bubbling with N_2 or CO_2 gas during the recycling experiments, measured at 10.0 ºC without glucose. The PBA@PM was simply separated by centrifugation, and reused directly for the next cycle. The yield of **6** were harvested after 96 hours' reaction.

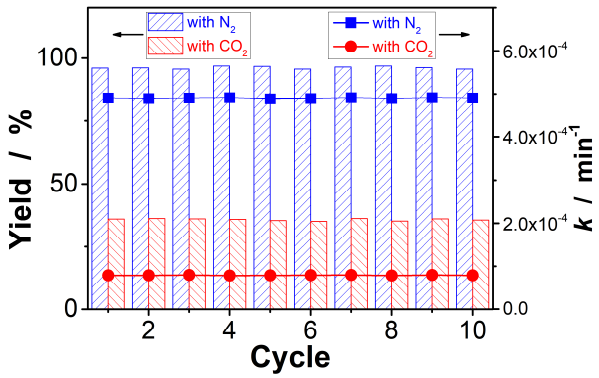

Fig. S22. A comparison of the catalysis activity of the PBA@PM upon bubbling with N_2 or CO_2 gas during the recycling experiments, measured at 10.0 ºC without glucose. The recycled PBA@PM was purified before reuse. The yield of **6** were harvested after 96 hours' reaction.

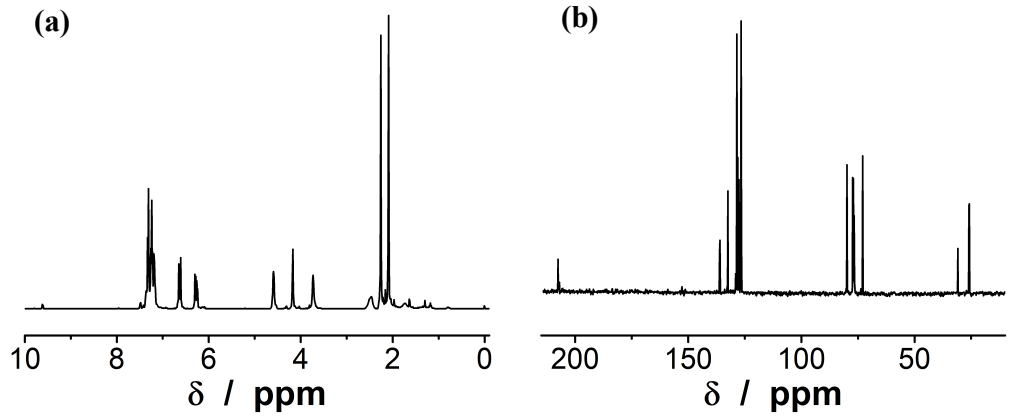

Fig. S23. (a) ^{1}H NMR (in $CDCl_3$) and (b) ^{13}C NMR (in $CDCl_3$) spectra of aldol adduct **7**. ^{1}H NMR: δ = 7.33-7.15 (5H), 6.62 (1H), 6.26 (1H), 4.61 (1H), 4.18 (1H), 3.74 (1H), 2.47 (1H), 2.25 (3H); ^{13}C NMR: δ = 207.5, 136.2, 132.5, 128.5, 128.1, 127.6, 126.9, 80.2, 72.8, 26.2.

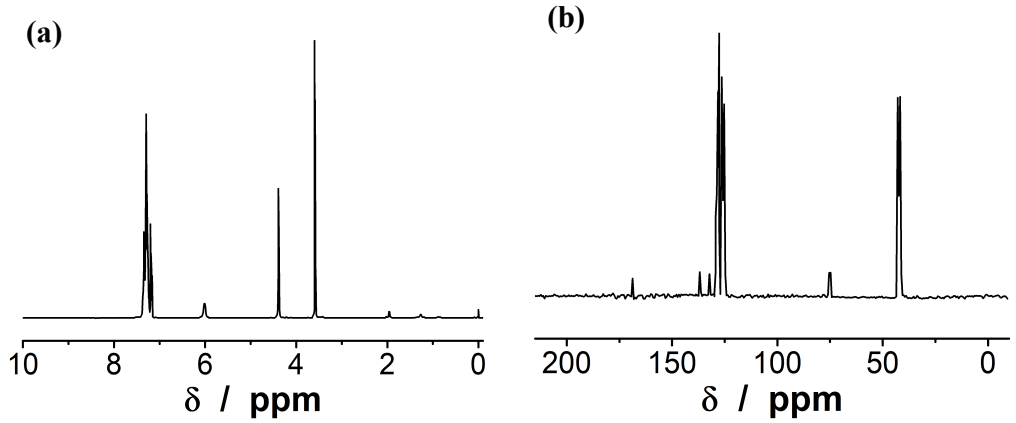

Fig. S24. (a) ^{1}H NMR (in $CDCl_3$) and (b) ^{13}C NMR (in $CDCl_3$) spectra of amide product **8**. ^{1}H NMR: δ = 7.33-7.15 (10H), 6.02 (1H), 4.37 (2H), 3.59 (2H); ^{13}C NMR: δ = 169.8, 137.2, 134.6, 129.3, 128.9, 128.5, 127.4, 127.3, 127.2, 43.6, 43.4.

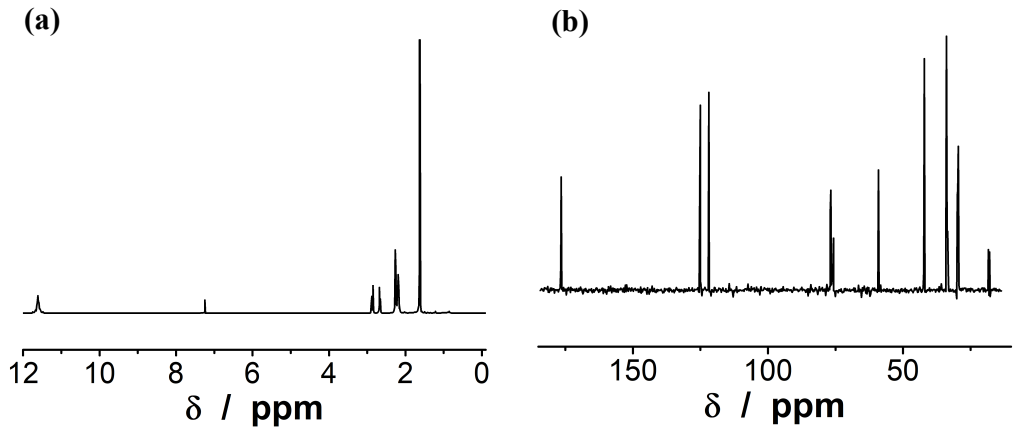

Fig. S25. (a) ^{1}H NMR (in $CDCl_3$) and (b) ^{13}C NMR (in $CDCl_3$) spectra of cycloadduct **9**. ^{1}H NMR: δ = 11.62 (1H), 2.85 (1H), 2.68 (1H), 2.27 (2H), 2.18 (2H), 1.63 (6H); ^{13}C NMR: δ = 177.3, 125.0, 122.7, 59.2, 43.0, 34.1, 30.3, 19.0, 18.6.

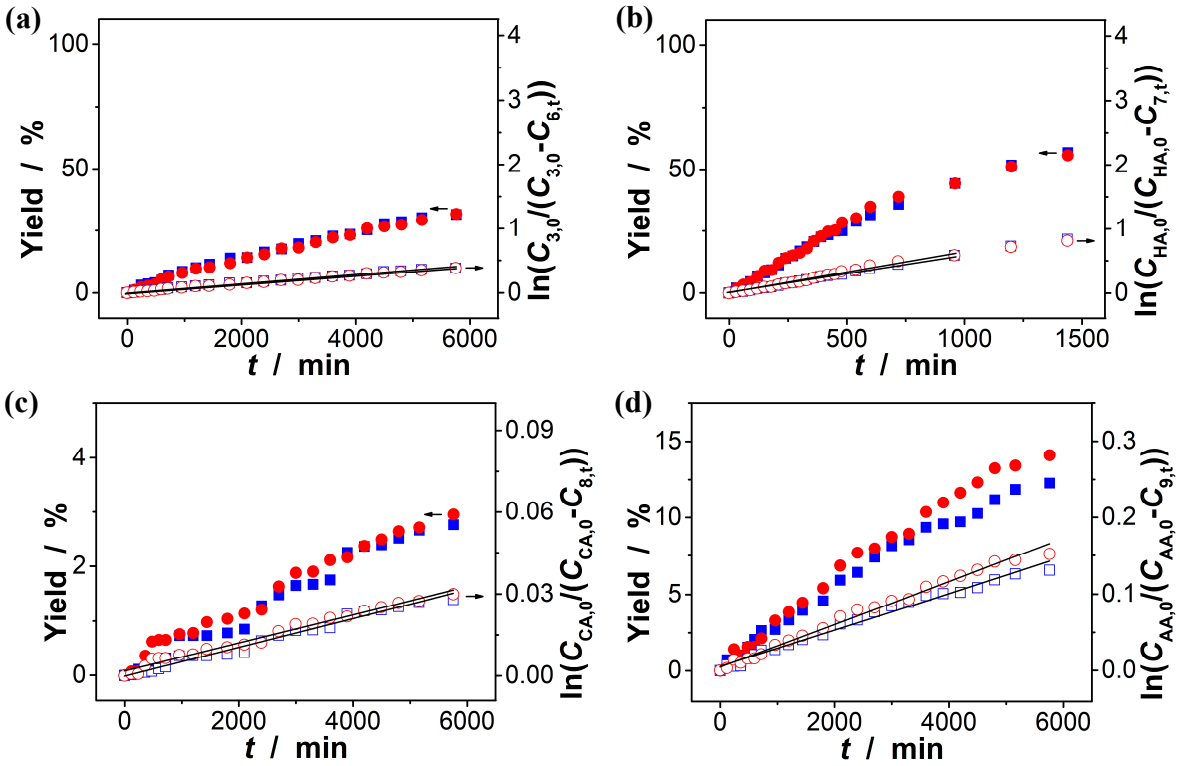

Fig. S26. Control experiments on the model (a) aza-Michael addition, (b) aldol, (c) amidation, and (d) [4+2] cycloaddition reactions catalyzed by **1**, upon bubbling with N_2 (■,□) or CO_2 (●,○) gas, and at 10.0 ºC, where lines are 1st-order kinetic fits.